An Analytical Study of the Redox Behavior of 1,10-Phenanthroline-5,6-dione, Its Transition-Metal Complexes, and Its *N*-Monomethylated Derivative with Regard to Their Efficiency as Mediators of NAD(P)$^+$ Regeneration

Gerhard Hilt, Tafeeda Jarbawi, William R. Heineman, and Eberhard Steckhan*

Abstract: The synthesis as well as the chemical and electrochemical properties of homoleptic and heteroleptic (trispyridylmethylamine as coligand) transition-metal complexes (Ru and Co) of 1,10-phenanthroline-5,6-dione (PD) and of its *N*-monomethylated derivative (PDMe$^+$) are described. In particular, their ability to abstract hydride ions was studied. Electrochemical investigations with cyclic voltammetry, rotating disk electrode experiments, and spectroelectrochemical methods at different pH values gave an insight into the complex electrochemistry of the compounds described, which is strongly influenced by a hydration pre-equilibrium. The electrochemically active quinone form of the transition-metal complexes can be reduced to the hydroquinone state in acidic solution and to their transition-metal-stabilized semiquinone states for neutral and basic solutions, whereas PDMe$^+$ is reduced to the hydroquinone state in both acidic and neutral solutions. The compounds can also be reduced chemically, and are efficient catalysts for the indirect oxidation of the enzymatic cofactor NAD(P)H. For the indirect aerobic NAD(P)H oxidation, up to 900 turnovers per hour can be observed, an achievement yet to be reached by other catalyst systems.

Keywords
catalysis · cobalt · cofactors · redox systems · ruthenium

Introduction

Enzymatic oxidation reactions can be of great value in organic synthesis.[1] Nature has developed a large number of highly selective oxidizing enzymes, among which monooxygenases like enzymes dependent on cytochrome P-450,[2] dioxygenases like the arene dioxygenases,[3] and oxidases like glycerol 3-phosphate oxidase[4] have found important applications in synthesis. The most widely employed class of oxidizing enzymes, however, are dehydrogenases like horse-liver alcohol dehydrogenase (HLADH).[5] These dehydrogenases depend on NAD(P)$^+$ as the electron-accepting cofactor. Thus, for synthetic application of these enzymes an efficient and mild system for cofactor regeneration is necessary.[1, 6] Apart from enzymatic cofactor recycling systems, chemical and electrochemical regeneration procedures have attracted great interest because of their greater flexibility. Chemical regeneration systems usually consist of *o*-quinoid mediators acting as hydride-ion abstracting agents and oxygen as the final electron acceptor. Catalase is added to destroy the hydrogen peroxide produced. Effective chemical regeneration systems must meet the following requirements: 1) To obtain a high yield in a reasonable time the turnover frequencies of the quinoid mediators must be as high as possible. 2) The mediators must be stable in both redox states within the regenerating cycle over a long period of time. 3) They should be easily soluble in the aqueous buffer systems necessary for enzymatic conversions. 4) They should react selectively only with the reduced cofactor.

Electrochemical regeneration of the oxidized cofactors is possible either by direct anodic oxidation[7] or by redox catalysts, also mainly applying *o*-quinoid systems as mediators. Alternative chemical systems described thus far are of limited use because they either react too slowly (flavine mononucleotide (FMN):[5, 8] 1.8 turnovers h^{-1}; 4,7-phenanthroline-5,6-dione:[9] 4–6 turnovers h^{-1}) or are not chemically stable enough under basic conditions,[10] which are usually favorable for the enzymatic oxidations.

For the direct electrochemical regeneration electrode fouling has been observed. Moreover, the anodic potential is too positive for selective oxidations[7] because of the electrochemically irreversible process. To solve these problems for the efficient chemical and electrochemical regeneration of NAD(P)$^+$, the 1,10-phenanthroline-5,6-dione system is a good starting point. However, the electron density within the *o*-quinoid structure

[*] E. Steckhan, G. Hilt
Institut für Organische Chemie und Biochemie der Universität Bonn
Gerhard-Domagk-Str. 1, D-53121 Bonn (Germany)
Fax: Int. code +(228)73-5683
e-mail: steckhan@uni-bonn.de
T. Jarbawi
Bir Zeit University Chemistry Department
P. O. Box 14, Ramallah, West Bank
W. R. Heineman
Department of Chemistry, University of Cincinnati
P. O. Box 172, Cincinnati, Ohio 45221-0622 (USA)

  0947-6539/97/0301-0079 $ 15.00+.25/0

should be diminished to accelerate the hydride transfer from NAD(P)H and to lower the oxidation potential for the electrochemical regeneration to about 0 V vs. Ag/AgCl in order to exclude side reactions of the substrates at the electrode surface. At the same time, the solubility should be enhanced by use of charged species, and the formation of insoluble precipitates by oligomerization of the reduced forms through hydrogen bonds should be avoided by blocking the nitrogen atoms. It was our strategy to solve all these problems by complexation of 1,10-phenanthroline-5,6-dione (PD) with a transition-metal ion[11] or by alkylation of the nitrogens. We have shown previously[11] that homoleptic complexes of Co^{II}, Ni^{II}, and Cu^{II} with 1,10-phenanthroline-5,6-dione do indeed undergo fast hydride transfers from NADH. However, the reduced forms of the complexes still precipitate slowly owing to oligomerization. In the case of Co^{II}, we could avoid the precipitation by using heteroleptic complexes in which four of the coordination sites were blocked by one *N,N,N*-tris(aminoethyl)-amine (tren) or *N,N,N*,-tris(pyridylmethyl)amine (TPA) ligand. In addition, the homoleptic tris-PD complex of Ru^{II} showed an extremely high stability even in the reduced form. Since these complexes are promising mediators for the NAD(P)$^+$ regeneration, we investigated their role in the cofactor regeneration systems, identified the active species involved in the process, and determined the number of active PD ligands in the above-mentioned tris-PD complexes. The following systems were studied (Scheme 1): 1) 1,10-phenanthroline-5,6-dione (PD) as the uncomplexed and unmodified model; 2) 1-methyl-1,10-phenanthrolinium-5,6-dione tetrafluoroborate ($PDMe^+$), an alkylated charged derivative of PD, as an alternative to the transition-metal complexes; 3) cobalt(II) trisphenanthroline $[Co^{II}(phen)_3]^{2+}$ as a typical reversible one-electron model; 4) the homoleptic complexes $[Co^{II}(PD)_3]^{2+}$ and $[Ru^{II}(PD)_3]^{2+}$; 5) the heteroleptic complexes $[Co^{II}(TPA)(PD)]^{2+}$ and $[Ru^{II}(TPA)(PD)]^{2+}$. We focused our investigations on the determination of the reduction and oxidation potentials, their pH dependence, and the number of transferred electrons and protons.

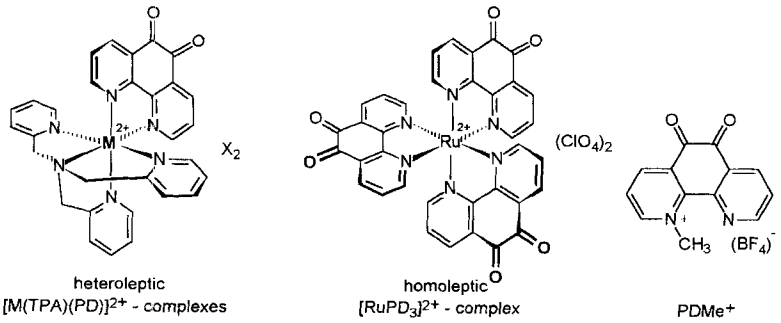

Scheme 1. Structures of the species studied.

The electrochemical behavior of PD has already been studied in water and in mixed aqueous media. Recently, Anson et al. published a study in which the compound was investigated mainly in acidic solutions.[12] Because enzymatic oxidations with NAD(P)$^+$-dependent alcohol dehydrogenases require basic aqueous phosphate buffer solutions, we mainly investigated the systems described above in the latter medium without any cosolvent present.

Abstract in German: *Die Synthese sowie die chemischen und elektrochemischen Eigenschaften homoleptischer und heteroleptischer (Tris(pyridylmethyl)amin als Coligand) Übergangsmetallkomplexe (Ru und Co) von 1,10-Phenanthrolin-5,6-dion (PD) und dessen N-monomethyliertes Derivat ($PDMe^+$) werden beschrieben. Insbesondere wurde deren Fähigkeit zur Abstraktion von Hydridionen untersucht. Für die elektrochemischen Untersuchungen wurden die Cyclovoltammetrie, Meßverfahren mit der rotierenden Scheibenelektrode und die Spektroelektrochemie unter Variation des pH-Wertes eingesetzt. Diese Studien gaben Aufschluß über die komplexe Elektrochemie der beschriebenen Verbindungen, die besonders durch ein vorgelagertes Hydratationsgleichgewicht bestimmt wird. In saurem Medium kann die elektroaktive Chinonform der Übergangsmetallkomplexe bis zur Hydrochinonform reduziert werden (zwei Elektronen pro PD-Einheit), während in neutralem und basischem Medium die Reduktion auf der Stufe des übergangsmetallstabilisierten Semichinons stehen bleibt (ein Elektron pro PD-Einheit). Dagegen wird $PDMe^+$ unter allen Bedingungen bis zur Stufe des Hydrochinons reduziert. Die Verbindungen können auch chemisch reduziert werden und sind wirksame Katalysatoren für die indirekte Oxidation des Enzym-Cofaktors NAD(P)H. Für die indirekte aeroben NAD(P)H Oxidation konnten bis zu 900 Cyclen pro Stunde festgestellt werden, ein Wert, der von anderen Katalysatorsystemen bisher nicht erreicht wurde.*

Results

Cyclic voltammetric studies: The cyclic voltammograms of the PD complexes and of $PDMe^+$ in the potential region between -0.4 and $+0.4$ V are comparable to those of free PD. The homoleptic ruthenium complex (Figure 1) shows only one redox pair for the noninteracting ligands, while the respective homoleptic cobalt complex shows splitting of the waves, of which two are distinguishable.

In the cyclic voltammograms, the reduction of complexed or free PD occurs in all compounds in the potential region of -0.2

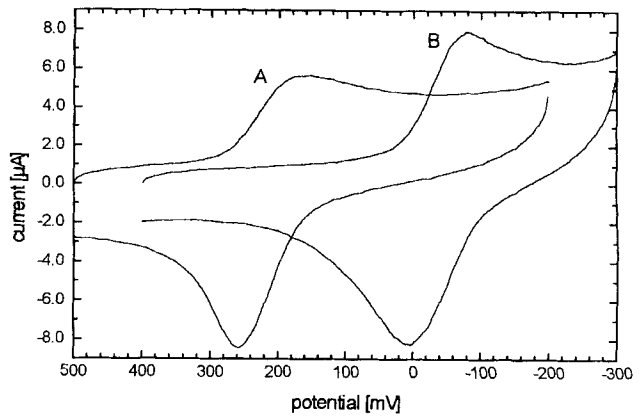

Fig. 1. Cyclic voltammograms of $[Ru(PD)_3](ClO_4)_2$ at pH 2.5 (A) and pH 7.4 (B) at a scan rate of 100 mVs^{-1} vs. Ag/AgCl reference electrode (working electrode: glassy carbon).

0947-6539/97/0301-0080 $ 15.00+.25/0 Chem. Eur. J. 1997, 3, No. 1

to +0.3 V vs. the Ag/AgCl reference electrode in a phosphate buffer. The shapes and potentials are strongly dependent on the pH value of the solution. The voltammograms in general show the behavior of a system with a preceding chemical reaction (C_rE_r) under total ($PDMe^+$) or intermediate (all other compounds) kinetic control in the more acidic region (Figure 1, curve A) and a more Nernstian behavior in the neutral and basic region (Figure 1, curve B) with the exception of PD. Above pH 3.6, the reduced PD precipitates from the solution, thus preventing the observation of a reoxidation peak. The preceding chemical equilibrium is especially noticeable in the case of $PDMe^+$, which between pH 2 and pH 6 shows a cyclic voltammogram of purely kinetic control (Figure 2, curve A) and a Nernstian response at pH 9.0 (Figure 2B). As expected for C_rE_r mechanisms, starting from a cyclic voltammogram that indicates strong kinetic control, the increase of the scan rate leads to a more Nernstian (peak-shaped) behavior because the preequilibrium becomes "frozen". The forward rate constant of the preequilibrium is too small to deliver noticeable amounts of the electroactive species within the time limits of the potential scan. This is demonstrated for $PDMe^+$ in Figure 3. At higher pH values in the neutral or basic regions the more Nernstian behavior of the cyclic voltammograms at lower scan rates can be explained by an increase in the forward rate constant of the preequilibrium. In this situation, the preequilibrium is established so fast that it falls into the time domain of the potential scan. This is demonstrated in Figure 2B (see also simulated voltammograms in Figure 9). Because Nernstian behavior dominates in the neutral-to-basic region we report the peak potential values for pH 7 (see Table 1).

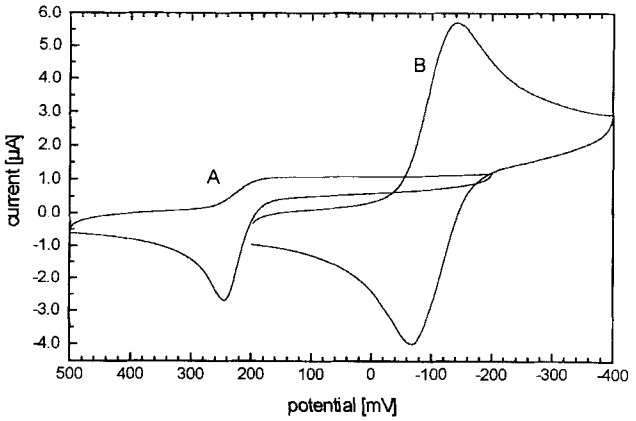

Fig. 2. Cyclic voltammograms of $PDMe^+$ at pH 2.4 (A) and pH 9.0 (B) at a scan rate of 20 mVs^{-1} vs. Ag/AgCl reference electrode (working electrode: glassy carbon).

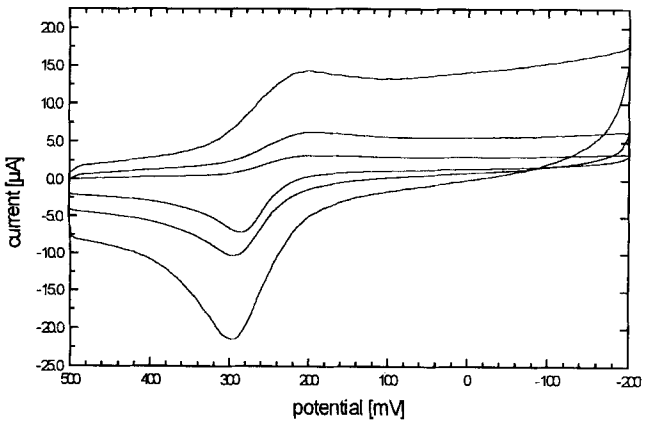

Fig. 3. Cyclic voltammograms of $PDMe^+$ at pH 2.5 and scan rates of 100, 400, and 1000 mVs^{-1} vs. Ag/AgCl reference electrode (working electrode: glassy carbon).

Table 1. Reductive ($E_{p,red}$) and corresponding oxidative ($E_{p,ox}$) peak potentials (V) at pH 7.0 and formal potentials ($E^{\circ\prime}$, V) in pH 2.5 and pH 7.0 or pH 8.0 phosphate buffer.

Compound	$E_{p,red}/E_{p,ox}$ [a] (pH)	$E^{\circ\prime}$ [b] (pH)
PD	−0.160/− (7.0)	−
$PDMe(BF_4)$	−0.005 [c]/+0.010 (7.0)	−
$[Ru(PD)_3](ClO_4)_2$	−0.060/+0.020 (7.0)	+0.242 (2.2)/−0.055 (8.0)
$[Co(TPA)(PD)](BF_4)_2$	−0.150/0 (7.0)	−0.040 (8.0)
$[Ru(TPA)(PD)](Cl)_2$	−0.110/−0.040 (7.0)	+0.217 (2.5)/−0.015 (7.0)

[a] Peak potentials from cyclic voltammograms at 20 to 100 mVs^{-1} scan rates. [b] Formal potentials taken from spectroelectrochemistry at OTTLE electrodes [c] Half peak potential (for 20 mVs^{-1}).

The cyclic voltammograms of the homoleptic cobalt complex $[Co(PD)_3](BF_4)_2$ show splitting of the waves, of which two are distinguishable. This indicates that the ligands are interacting within the complex. The two redox pairs for the ligands could be better resolved by means of differential pulse voltammetry giving redox potentials of $E_1 = +0.009$ V and $E_2 = -0.086$ V at pH = 7.0.

Because of the involvement of protons in the redox reaction, all peak potentials are shifted to more negative potentials with increasing pH. The amounts of these shifts were studied between pH 2 and pH 9. The reduction of the uncomplexed PD is chemically irreversible above pH 3.6. This has been observed before by Bruice et al.[13] and can be explained by the formation of precipitates of the reduced form owing to hydrogen-bond formation between the hydroxy groups of the hydroquinone and the nitrogen atoms. Therefore, the pH dependence of the peak potentials of PD can only be determined for the reduction process.

In the transition-metal complexes of PD as well as in the *N*-methylated form $PDMe^+$, the nitrogen atoms are blocked so that the precipitation of the hydroquinone forms through hydrogen bonding between the hydroxy groups and the nitrogens is prevented. Therefore, here the pH dependence of both reduction and oxidation potential can be observed even under neutral or basic conditions. We found a linear correlation between the anodic peak potential and the pH with slopes of approximately −52 mV per pH unit between pH 2 and pH 9 for all observed compounds. The pH dependence of the cathodic peak potentials of all compounds has three different regions (see Table 2). In the first region between pH 2 and pH 4 to pH 4.5, linear correlations between the peak potentials and the pH with slopes of around 90 mV per pH are observed. For $[Co(PD)_3]^{2+}$ reliable data could not be obtained because the cyclic voltammograms are poorly developed. In the second region betweeen pH 4.0 to pH. 4.5 and about pH 7, linear correlations between the peak potentials and the pH with slopes of around 30 mV per pH unit are obtained. Exceptions are $PDMe^+$ and the heteroleptic complex-

Table 2. pH dependence of cyclic voltammetric peak potentials. Slopes for separate regions are given in mV per pH unit, with the end point of the pH region in brackets; the slope for the reoxidation is given for the whole region in mV.

Compound	Reduction Region 1	Region 2	Region 3	Reoxidation Whole pH region
PD	−96 (4.0)	−29 (8.0)	decomp.	irreversible
$PDMe(BF_4)$	−93 (4.5)	−49 (7.4)	−72 (9.0)	−50
$[Ru(PD)_3](ClO_4)_2$	−85 (4.2)	−30 (6.2)	−52 (9.0)	−51
$[Co(TPA)(PD)](BF_4)_2$	−84 (4.3)	−62 (9.0)	−62 (9.0)	−52
$[Ru(TPA)(PD)](Cl)_2$	−90 (4.2)	−14 (6.6)	−52 (11.0)	−54

es with values of 50 mV. The third basic region between about pH 7 to pH 9 shows slopes of around 50 mV per pH unit. A typical example is given for $[Ru(PD)_3]^{2+}$ in Figure 4. Again $PDMe^+$ is an exception with a slope of 72 mV. The cyclic voltammogram of the uncomplexed PD is strongly influenced by the decomposition of the substrate at these pH values. Measurements in buffer systems above pH = 9.0 are not possible for most of the complexes; only the heteroleptic ruthenium complex $[Ru(TPA)(PD)]^{2+}$ was stable up to pH 11.

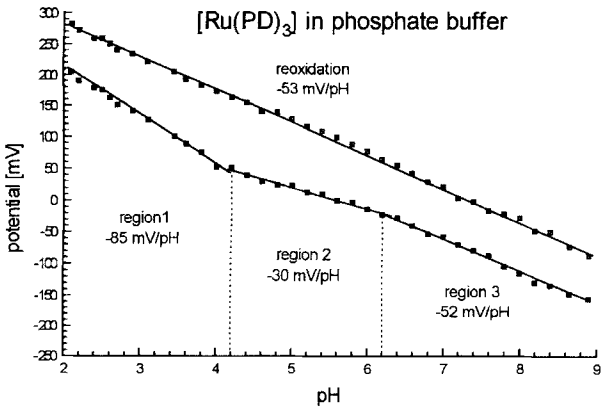

Fig. 4. pH dependence of the reductive and oxidative peak potentials of $[Ru(PD)_3](ClO_4)_2$ measured by cyclic voltammetry at a scan rate of 100 mVs^{-1} vs. Ag/AgCl reference electrode (working electrode: glassy carbon).

Rotating disk electrode measurements: Rotating disk electrode measurements allow the determination of the number of transferred electrons and/or the diffusion coefficients, if the redox process is a simple diffusion-controlled electron transfer. This results in a linear Levich plot of the plateau current vs. the square root of the rotation rate.[14] If, however, the redox process is perturbed by preceding or follow-up chemical and electrochemical steps, nonlinear Levich plots are obtained. Preceding chemical equilibria especially can very often easily be detected by this experiment. This is of considerable importance in the case of the compounds studied here, because Anson et al.[12] have shown that protonation or complexation of PD by metal ions leads to the partial formation of electrochemically inactive hydrated PD ($PD-H_2O$). In the case of PD, the hydration occurs only when a nitrogen is protonated in the region below pH 5, thus lowering the electron density of the dione system. Such a preequilibrium influences the plateau currents. The Levich plot therefore deviates from linearity; the slope decreases and finally at high rotation rates the current becomes independent of the rotation rate.[15] This preequilibrium should also be expected in the case of the compounds studied here.

Like the proton in the case of the uncomplexed PD, not only the transition-metal ions in the complexes but also the methyl group in $PDMe^+$ should strongly favor hydrate formation at higher pH values as well. We therefore studied all the compounds by rotating disk measurements at pH 2.2 or pH 2.5 and pH 7.0 at rotation rates between 100 and 10000 rpm and compared them with the stable and reversible system $[Co(phen)_3]^{2+}$. For the cobalt trisphenanthroline model system, the Levich plot was a straight line through the origin. At pH 2.2 or pH 2.5, linear Levich plots were also observed for all other compounds between 100 and 10000 rpm. The extrapolations of the lines, however, cut the current axis at positive current values. At pH 7, the plots deviated from linearity: the slopes decreased with increasing rotation rates in accordance with the model discussed above. Again, the extrapolation of the curves to a rotation rate of 0 rpm did not pass through the origin. Typical examples are given for $[Ru(PD)_3]^{2+}$ and $PDMe^+$ in Figures 5 and 6. The Levich plots for $PDMe^+$ resembled the Levich plots of the other compounds; however, the cathodic plateau currents were much smaller than for $[Ru(PD)_3]^{2+}$.

The number of transferred electrons could not be determined by this experiment because the amount of electroactive material depends on the equilibrium between the hydrated and the nonhydrated forms and is therefore unknown.

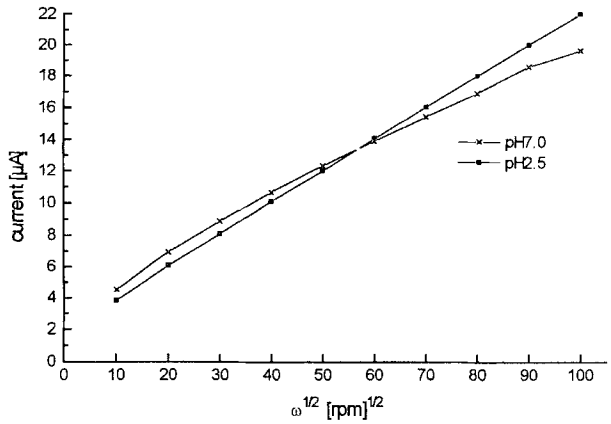

Fig. 5. Levich plots of the cathodic plateau currents of $[Ru(PD)_3](ClO_4)_2$ (2.34×10^{-4} mol L^{-1}) at pH 2.5 and pH 7.0.

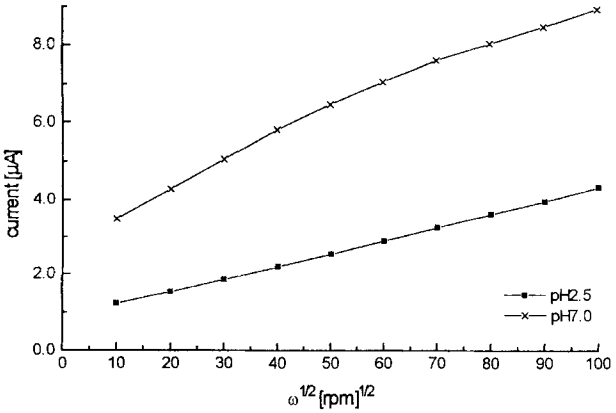

Fig. 6. Levich plots of the cathodic plateau currents of $PDMe^+$ (5.02×10^{-4} mol L^{-1}) at pH 2.5 and pH 7.0.

0947-6539/97/0301-0082 $ 15.00+.25/0 Chem. Eur. J. 1997, 3, No. 1

Determination of the total number of electrons: From the voltammetric data only the ratio of transferred protons to electrons can be obtained. The absolute number of electrons consumed in the overall process can very easily be established by exhaustive controlled potential electrolysis or spectroelectrochemical experiments within an optically transparent thin-layer electrochemical (OTTLE) cell[19] (see below).

Exhaustive controlled potential electrolysis: Using exhaustive controlled potential electrolysis at potentials slightly more negative than the reduction peak potential, we measured the total number of transferred electrons under acidic conditions at pH 2.2 and under neutral or slightly basic conditions at pH 7 or pH 8 (see Table 3). At pH 2.2 two electrons per phenanthroline-dione unit were transferred in all cases, giving a total number of six electrons for the homoleptic complexes. At pH 7 or pH 8, however, only one electron for each PD unit was transferred, with the exception of $PDMe^+$, for which a two-electron transfer occurred. During exhaustive electrolysis of PD, precipitates formed as mentioned above. Therefore, the values for PD are of questionable validity. Similarly, small amounts of precipitates formed for $[Co(PD)_3]^{2+}$ at pH 8.0.

Table 3. Number of transferred electrons during exhaustive controlled potential electrolysis at different pH values.

Compound	Number of electrons (pH)
PD	1.98 (2.2)/0.99 (8.0)
$PDMe(BF_4)$	1.99 (2.2)/2.03 (7.0)
$[Co(phen)_3](BF_4)_2$	0.99 (8.0)
$[Co(PD)_3](BF_4)_2$	5.99 (2.2)/2.96 (8.0)
$[Ru(PD)_3](ClO_4)_2$	5.89 (2.2)/2.91 (8.0)
$[Co(TPA)(PD)](BF_4)_2$	1.96 (2.2)/0.91 (7.0)
$[Ru(TPA)(PD)](Cl)_2$	2.14 (2.2)/1.03 (7.0)

Spectroelectrochemical study in an OTTLE cell: As shown by Heineman et al.,[19] spectroelectrochemical studies with an optically transparent thin-layer electrode can easily be used to determine the redox potentials and the number of transferred electrons from a Nernst plot of the applied equilibrium potentials versus the log[Ox]/[Red]. The ratio of the concentrations of oxidized and reduced forms are obtained from the ratio of the absorbance values for the oxidized and reduced forms at any UV/vis wavelength other than the isosbestic points. In our case absorption maxima at wavelengths around 250 nm (pH 2.2 and pH 2.5) or 264 nm (pH 7.0) for the PD ligand were used. At the same time, the UV/vis spectra obtained in this way can give more information about the nature of the oxidized and reduced forms of the compounds. All spectroelectrochemical measurements show clear isosbestic points, indicating that one species is transformed to only one other species. Typical spectroelectrochemical measurements at pH 2.2 and pH 7.0 are given for $[Ru(PD)_3]^{2+}$ in Figures 7A and 7B. The experiments failed for PD and $PDMe^+$ because the reduced form of PD precipitated during the electrochemical conversion within the thin-layer cell while the reduction of PDME above potentials of -80 mV vs. Ag/AgCl produced a blue solution from which brownish-yellow needles crystallized at the minigrid electrode, and further transformation became impossible. Also for the reduced form of the $[Co(PD)_3]^{2+}$ complex crystals were formed at pH 7.0 after a period of time. All measurements yielded linear Nernst plots (Table 4).

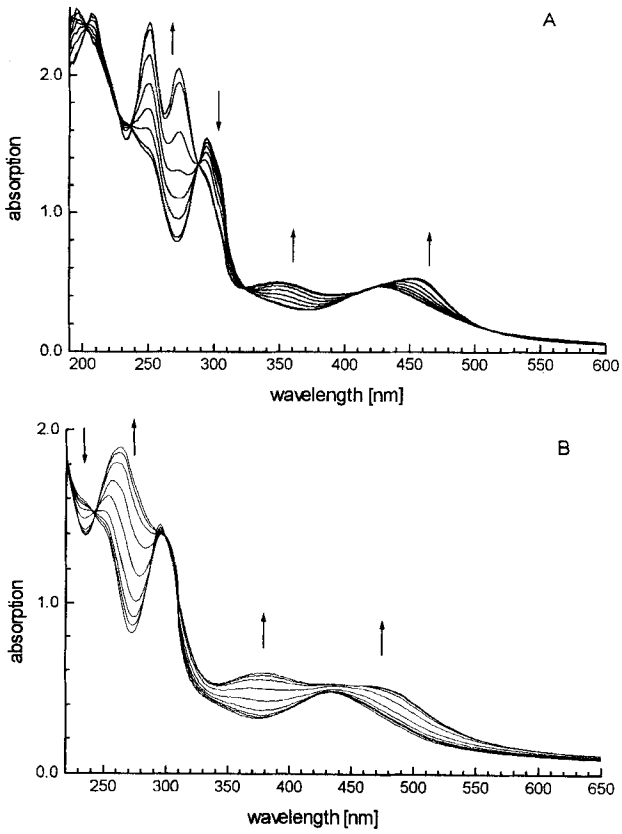

Fig. 7. UV/vis spectral changes during the electrochemical reduction of $[Ru(PD)_3](ClO_4)_2$ at an OTTLE at pH 2.2 (A) and at pH 7.0 (B) for 350, 280, 260, 250, 240, 230, 210, 150 mV (A) and 100, 50, 30, 10, −10, −30, −50, −70, −100 mV (B) vs. Ag/AgCl reference electrode. The arrows in the Figures indicate the direction of the change of the spectra during stepwise reduction of the PD complexes.

Table 4. Slopes of the plots of the applied potentials versus log[Ox]/[Red] from spectroelectrochemical measurements in the OTTLE cell.

Compound	Slope at pH 2.5	Slope at pH 7.0
$[Co(phen)_3](BF_4)_2$	–	−60 (pH 8.0)
$[Co(PD)_3](BF_4)_2$	−24	−60
$[Ru(PD)_3](ClO_4)_2$	−29 (pH 2.2)	−55
$[Co(TPA)(PD)](BF_4)_2$	–	−58
$[Ru(TPA)(PD)](Cl)_2$	−31	−52

At pH 2.5, the metal complexes gave a slope of the Nernst plot of around 29 mV, indicating a transfer of two electrons per PD unit. At pH 7.0 or 8.0, the slopes were all around 60 mV showing a transfer of only one electron per PD unit. The results for the metal complexes therefore agree very well with those of the exhaustive controlled potential electrolyses.

Study of the chemical reduction of the PD transition-metal complexes by NADH and $NaBH_3CN$: As it is our aim to use the PD transition-metal complexes and $PDMe^+$ as effective hydride-ion abstracting agents towards the chemical aerobic or indirect

electrochemical regeneration of $NAD(P)^+$ from NAD(P)H in enzymatic syntheses, we studied the rate of the aerobic PD transition-metal complex and $PDMe^+$-catalyzed generation of NAD^+ from NADH (Scheme 2). We found that our previously reported values for some of the complexes[11] could actually be increased considerably by changing the pH from 6.0 to pH 8.0 (Table 5). This is advantageous because most of the enzymatic

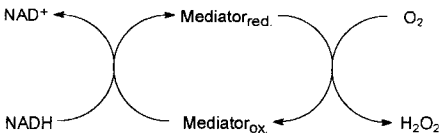

Scheme 2. Reaction path for the aerobic NADH oxidation.

Table 5. Turnover frequencies (TNh^{-1}) for the aerobic generation of NAD^+ from NADH with PD-based catalysts.

Compound	TNh^{-1} [a], pH 6.0	TNh^{-1} [a], pH 8.0
$[Ru(PD)_3](ClO_4)_2$	55	900
$[Ru(TPA)(PD)](Cl)_2$	31	737
$[Co(TPA)(PD)](BF_4)_2$	23	96
$PDMe(BF_4)$	33	96

[a] Turnover number for the PD catalyst per hour.

oxidations catalyzed by alcohol dehydrogenases are favored by basic conditions. While at pH 6.0 the rate reaches 55 turnovers of the PD-based catalyst per hour, the rate increases to up to 900 turnovers per hour at pH 8.0. The free PD alone is almost totally ineffective and in addition the reduced form precipitates from the solution. Therefore, we are presenting here the most efficient catalysts for the NAD^+ regeneration known up to now. All the catalyst systems used here were totally stable during the reaction time. No precipitation occured.

The electrochemical reoxidation of the reduced mediator was also possible, so that for preparative applications of the mediators in enzymatic systems the regeneration system O_2/catalase can be substituted by an anode. Within the test system NADH/mediator/anode, smaller turnover numbers compared with the aerobic reoxidation are observed (Table 6). This can be explained by the heterogeneity of the charge transfer, which is limited by diffusion and the surface area of the anode. Under electrochemical conditions too the mediators were totally stable.

Table 6. Turnover frequencies (TNh^{-1}) for the electrochemical generation of NAD^+ from NADH with PD-based catalysts.

Compound	TNh^{-1} at pH: 6.0	7.0	7.9
$[Ru(PD)_3](ClO_4)_2$	30	35	39
$[Ru(TPA)(PD)](Cl)_2$	23	21	21
$PDMe(BF_4)$	34	36	35
$[Co(TPA)(PD)](BF_4)_2$	24	20	26

Within the context of this study, we wanted to investigate whether the electrochemical reduction studied by spectroelectrochemistry was generating the same reduced species as the ones obtained by reaction with NADH. Because NADH and NAD^+ themselves absorb in the UV/vis region in which the reduced PD systems can be observed, we used $NaBH_3CN$, assuming that this reagent would also react as a hydride-ion transfer agent.

The UV/vis spectra that we obtained during reduction with $NaBH_3CN$ at pH 2.2 and at pH 7.0 (Figure 8A,B) are indeed identical to those which we obtained at the same pH values by the spectroelectrochemical measurements (Figure 7A,B). The total reduction by $NaBH_3CN$ at pH 2.2 took place at a considerably faster rate (4 min) as compared with the reduction at pH 7.0 (36 min). Some data for the UV/vis spectra are given in Table 7. During the reduction at pH 7.0 one new intensive band at 260–280 nm is generated, while at pH 2.5 two intensive bands are growing between 240–300 nm.

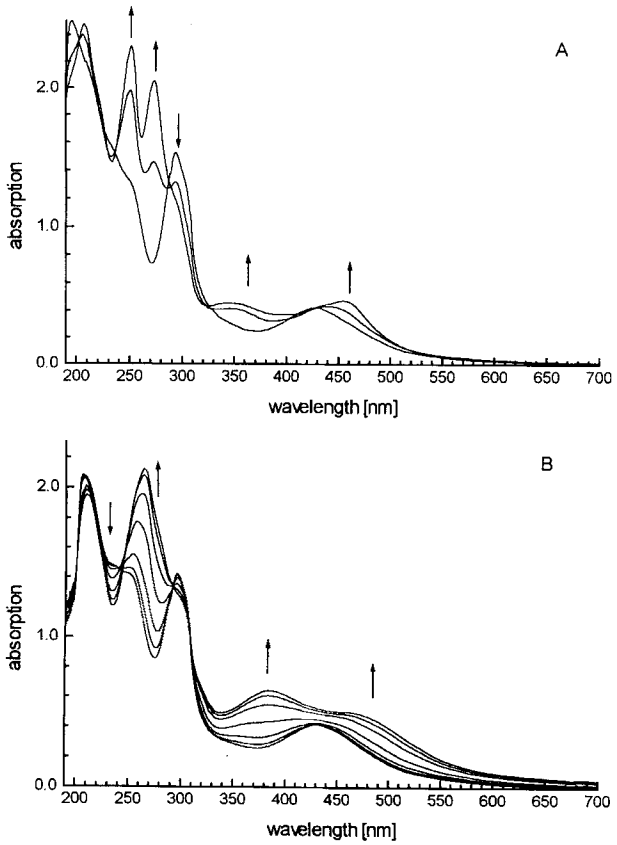

Fig. 8. UV/vis spectral changes during the chemical reduction of $[Ru(PD)_3](ClO_4)_2$ by $NaBH_3CN$ at pH 2.2 with 0, 2, and 4 min reaction time (A) and pH 7.0 with 0, 6, 12, 18, 24, 30, and 36 min reaction time (B).

Discussion

The interpretation of the Nernst–Clark plots of the cyclic voltammetric peak potentials versus solution pH is complicated by the fact that the electrochemical processes are governed by a preceding equilibrium between the electrochemically active PD compound and its electrochemically inactive hydrated form, as has recently been described by Anson et al. (see Scheme 3).[16] The rate of the establishment of the equilibrium is obviously

0947-6539/97/0301-0084 $ 15.00+.25/0 Chem. Eur. J. 1997, 3, No. 1

Table 7. UV/Vis maxima of the oxidized and reduced compounds at different pH values (sh = shoulder).

Compound	Oxidized form		Reduced form	
	pH 7.0	pH 2.5	pH 7.0	pH 2.5
PD [a]	–	254/315	–	254/295/350sh
$[Co(phen)_3](BF_4)_2$	200/226/275	–	205/220/272/280	–
$[Co(PD)_3](BF_4)_2$	197/253/300/309	195/252/302	197/254/290/340sh	213/**260**/**295**/350sh
$[Co(TPA)(PD)](BF_4)_2$	199/222sh/287/340	–	200/222sh/**282**/340	–
$[Ru(PD)_3](ClO_4)_2$	200/250sh/296/431	195/250sh/294/430	200/210sh/**265**	207/**250**/**273**/295sh
			300sh/382/489	352/455
$[Ru(TPA)(PD)](Cl)_2$	200/245/296/350	200/245/296/350	200/249/**264**/296/352	200/**249**/**274**/292sh/343

[a] Compare ref. [12]: electrolyses in 0.1 M CF_3SO_3H.

influenced by the pH (see below); this results in more Nernstian behavior of the cyclic voltammograms at higher pH values. Therefore, changes in the pH influence the peak potentials not only through the number of protons which are involved in the electrochemical step but also to a certain extent by the pH influence on the rate constants of the preequilibrium. The reoxidation peaks, however, are less influenced by the preequilibrium.

The peak potential shift of about 90 mV per pH unit between pH 2.2 and pH 4.0–4.5 (region 1, Table 2) can normally be explained by an uptake of two electrons and three protons during the electrochemical experiment. For PD, this result is in accordance with the recently published results of Anson et al.,[12] assuming the formation of the *N*-protonated hydroquinone form under acidic conditions up to pH 4.0. The slope of 29 mV per pH unit between pH 4.0 and pH 8.0 (region 2, Table 2) for PD can be explained by the uptake of two electrons and one proton, thus forming the deprotonated hydroquinone form indicated in Scheme 3.

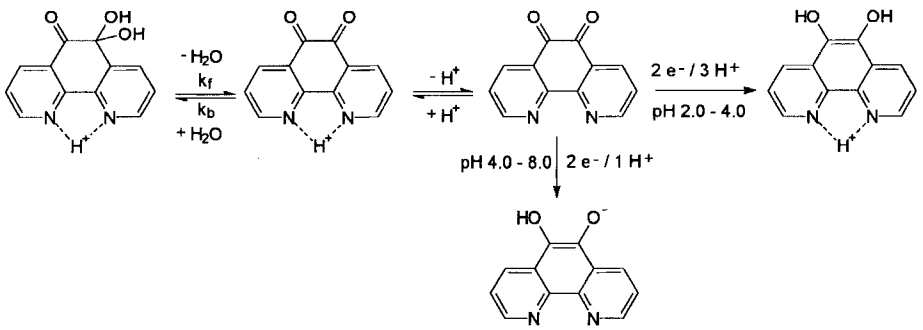

Scheme 3. Electrochemical behavior of uncomplexed 1,10-phenanthroline-5,6-dione in phosphate buffers of different pH.

In the acidic region 1, the behavior of the PD transition-metal complexes can be explained quite similarly if one assumes only a small influence of the preequilibrium on the peak potential shift. Under this condition it can be concluded that the electrochemical reduction leads to a protonated hydroquinone transition-metal complex (two electrons, three protons). Because the nitrogens are blocked by the transition metal the protonation must occur at the oxygens, as indicated in Scheme 4. The slope of about 52 mV per pH unit in region 3 for most of the PD transition-metal complexes can either be explained by a two-electron/two-proton or a one-electron/one-proton process. The change from a two-electron/one-proton process at pH values up to about 7.0 to a two-electron/two-proton process at more basic pH does not seem to be logical. Therefore, we investigated the number of transferred electrons independently from cyclic

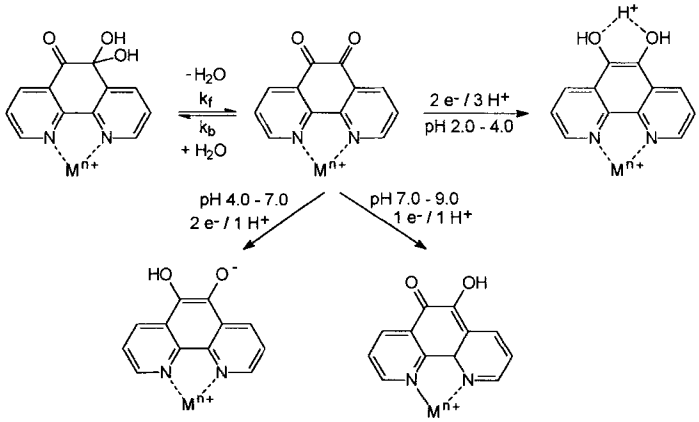

Scheme 4. Electrochemical behavior of 1,10-phenanthroline-5,6-dione transition-metal complexes in phosphate buffers of different pH.

voltammetry by exhaustive controlled potential electrolysis and by spectroelectrochemical measurements. Both measurements yielded the same total number of electrons. Under acidic conditions at pH 2.2 or 2.5, two electrons for each PD unit of the complex are transferred, while at pH values above about 7.0 only one electron per PD unit is transferred, with the exception of $PDMe^+$. This could best be rationalized by a stabilization of the semiquinone complex by the transition-metal ion, leading to an increase of the coordinative binding order of the metal under basic conditions. In an acidic medium the protonation of the semiquinone complex at the carbonyl group would favor the further reduction to the hydroquinone complex (Scheme 5). The stabilization of protonated semiquinones by metal ions has already been proposed.[17] Because such a stabilization is impossible in the case of $PDMe^+$, two-electron processes are found for both acidic and basic conditions.

The UV/vis spectra obtained by spectroelectrochemical reduction in an OTTLE cell and by chemical reduction with $NaBH_3CN$ (shown in Figure 7 and Figure 8) are identical. However, under acidic and basic conditions two different species are formed, as already pointed out in the preceding discussion. Under acidic conditions, the spectra can be attributed to the hydroquinone complexes. However, it is not possible to distinguish between hydroquinone/quinone dimers and semiquinone complexes in the spectra under basic conditions. Be-

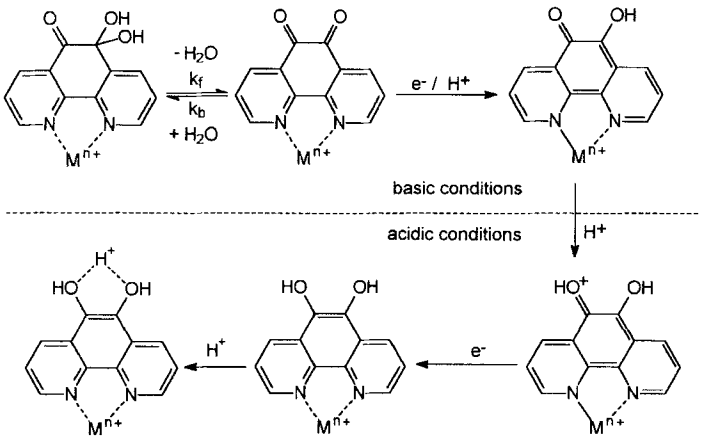

Scheme 5. Possible one-electron/one-proton process under basic conditions and two-electron/three-proton process under acidic conditions.

sides being hydride transfer agents, borohydrides can act as effective single-electron reducing agents leading to semiquinone metal complexes (Bock[17]). Thus, our first assumption that the borohydride would only react as a hydride-ion transfer agent might not hold for basic conditions. The formation of the semiquinone complexes can also be rationalized easily by the comproportionation of the hydroquinones initially formed by hydride-ion transfer and the starting quinone systems to generate the semiquinone complexes (Scheme 6).

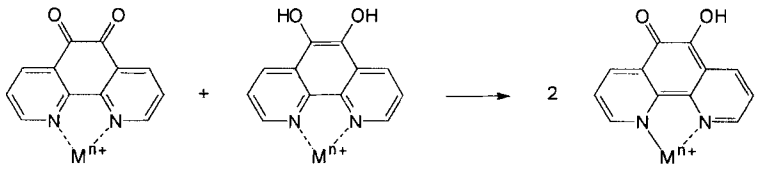

Scheme 6. Comproportionation of quinone and hydroquinone complexes to give the protonated semiquinone complex.

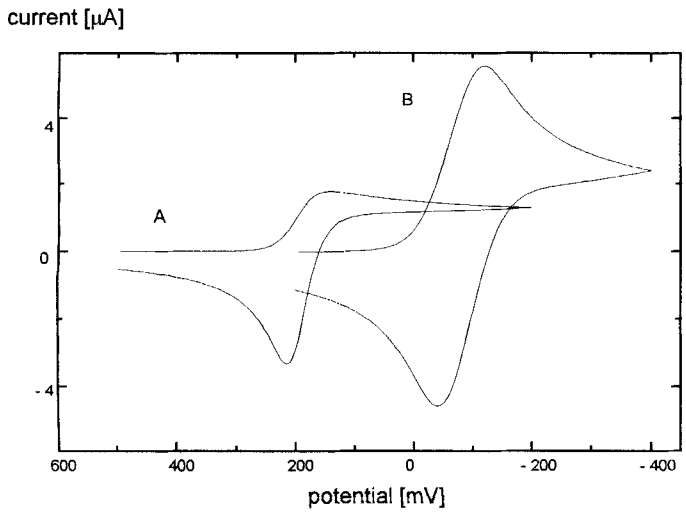

Fig. 9. Digital simulation of the cyclic voltammograms of $PDMe^+$ at pH 2.5 (A) and pH 9.0 (B). Applied mechanism: A + e = B; B + e = C; D = A with A = $PDMe^+$; B = $PDMe^+$ semiquinone; C = $PDMe^+$ hydroquinone; D = electroinactive $PDMe^+$ hydrate. For pH 2.4, $E_1 = E_2 = 250$ mV and $k_f = 0.15\ s^{-1}$, $K_{eq} = 0.1$; for pH 9.0, $E_1 = 0$ and $E_2 = -100$ mV and $k_f = 25\ s^{-1}$, $K_{eq} = 0.1$. The α values were set to 0.5, the heterogeneous standard electron-transfer rate constant was 1×10^2 cm s^{-1} and all diffusion coefficients 1×10^{-5} $cm^2 s^{-1}$.

The rotating disk electrode measurements together with the cyclic voltammetric measurements clearly indicated the hydration preequilibrium of the PD complexes and of $PDMe^+$. The cyclic voltammograms became more Nernstian with increasing scan rate and also with increasing pH. The Levich plots were curved under basic conditions and gave straight lines that intersected the current axis at positive values for acidic conditions. These observations can only be brought into agreement under the following assumptions. The equilibrium constants k_f/k_b (Scheme 4) must be between 1 and 0.005 and the forward rate constant for the formation of the nonhydrated electroactive PD complex must be very small under acidic conditions. A digital simulation of the cyclic voltammograms (Figure 9) with DIGISIM software (DigiSim® 2.0, Bioanalytical Systems) for $PDMe^+$ at pH 2.5 gave as optimum values 0.1 ± 0.1 for the equilibrium constant between the hydrated and the nonhydrated forms and $0.15 \pm 0.05\ s^{-1}$ for the forward rate constant k_f for the dehydration step. The reduction takes place in one step at +0.25 V. With increasing pH the forward rate constant is increased; thus the preequilibrium is established faster and therefore a more Nernstian (peak-shaped) behavior is observed. Digital simulation of the reduction of $PDMe^+$ at pH 9.0 resulted in the same equilibrium constant of 0.1 ± 0.1 but a more than hundredfold higher forward rate constant of about $25 \pm 5\ s^{-1}$. The reduction of the nonhydrated form takes place in two steps, which are separated by 100 mV ($E_1 = 0.0$ V, $E_2 = -0.1$ V). The simulated voltammograms in Figure 9 compare extremely well with the measured cyclic voltammograms in Figure 2. The results from the rotating disk electrode may be interpreted in a similar way. At acidic pH the very slow equilibrium is "frozen" by the rotation rate and leads to a straight line of the Levich plot above 100 rpm. At neutral or slightly basic pH the equilibrium is reached faster and therefore a deviation from the straight line can be observed.

Higher turnover frequencies of the PD catalyst systems during the aerobic generation of NAD^+ from NADH at pH 8.0 as compared with pH 6.0 can be effected in two ways. First, the faster preequilibrium between the hydrated and nonhydrated PD complexes under basic conditions increases the turnover frequency. Secondly, because of the lower formal redox potentials of the catalysts under basic conditions the reoxidation of the hydroquinone or semiquinone system by oxygen should proceed faster. It seems, however, to be contradictory that the reduction by $NaBH_3CN$ is slower under basic conditions. This can be explained by the fact that the redox potentials under basic conditions are strongly shifted to more negative values, thus making the one-electron reduction by $NaBH_3CN$ less favorable. This, however, would only be effective if $NaBH_3CN$ reacts as a single-electron-transfer reducing agent and not as a hydride transfer agent.

Taking all our results into account, the efficient aerobic catalytic generation of NAD^+ from NADH under basic conditions employing the newly developed transition-metal complexes as redox catalysts may be rationalized as shown in Scheme 7. Hydride transfer from NADH to the PD transition-metal complex leads to the hydroquinone stage. Comproportion with the quinone results in the formation of two semiquinone

0947-6539/97/0301-0086 $ 15.00+.25/0 Chem. Eur. J. 1997, 3, No. 1

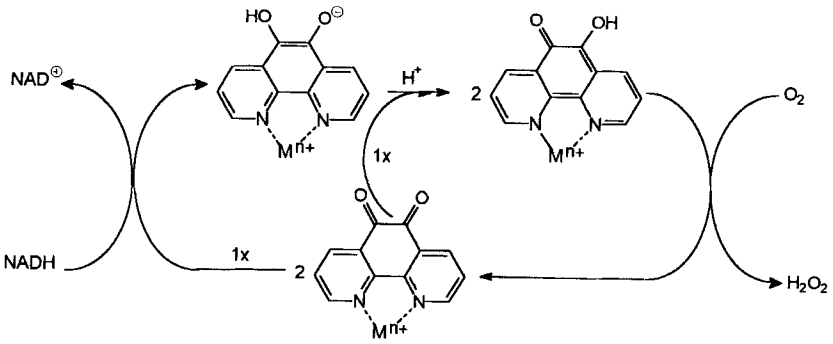

Scheme 7. The aerobic catalytic generation of NAD^+ from NADH under basic conditions employing the newly developed transition-metal complexes as redox catalysts.

species, which are subsequently oxidized by oxygen, forming hydrogen peroxide. Similarly, the oxidation can take place at the anode.

Conclusion

The three phenanthrolinedione transition-metal complexes, $[Ru(PD)_3]^{2+}$, $Ru(TPA)(PD)]^{2+}$, and $Co(TPA)(PD)]^{2+}$, and the *N*-methylated PD derivative $PDMe^+$, which have been synthesized and characterized, are very effective catalysts for the chemical aerobic and indirect electrochemical anaerobic generation and regeneration of NAD^+ from NADH. Thus, we have been successful in fulfilling the four requirements for an effective NAD^+ regeneration system: the turnover frequencies of up to 900 cycles per hour for the catalysts, especially for the ruthenium systems, are by far the highest ever reached. All systems are stable over the long term, especially the heteroleptic ruthenium complex, which is even stable at pH 11. Because of their charge, all systems are highly soluble in aqueous buffer solution. Their redox potentials are around 0 V and therefore the systems are very selective oxidizing reagents towards NADH. By careful study of the electrochemical properties it could be demonstrated that the redox behavior of the systems is quite different in acidic and basic buffer solutions. While in acidic solution two electrons are transferred to each PD ligand, under basic conditions only one electron per PD unit is exchanged. As shown by spectroscopy and spectroelectrochemistry, chemical and electrochemical reductions lead to the same reduced species. In addition, the hydration preequilibrium of the PD systems, which influences the reduction process, is also dependent on the pH of the buffer solution. Thus, at higher pH the equilibrium is faster than at lower pH. We are currently employing the mediators very successfully as catalysts for the cofactor regeneration in enzymatic syntheses that use alcohol dehydrogenases.[18]

Experimental Section

Instrumentation: The voltammetric investigations were carried out on BAS-100 B/W Electrochemical Analyzer and RDE-1 systems, Bioanalytical Systems (West Lafayette, Indiana, U. S. A.). Potentials were measured against the Ag/AgCl reference electrode BAS RE-5 (3 M NaCl); glassy carbon working electrodes (3 mm diameter) as well as Sigraflex® carbon foil electrodes (6 or 25 cm^2) were used for exhaustive controlled potential electrolysis experiments. For spectroelectrochemical experiments we used an optically transparent thin-layer electrode (OTTLE) system with a gold minigrid working electrode (500 wires/inch) as described by Heineman et al. [19]. UV/vis spectra were recorded with a Cary 1 UV/visible spectrophotometer (Varian, Palo Alto, California, U. S. A.) and IR spectra were recorded on an FT-IR 1600 spectrometer (Perkin–Elmer, Überlingen, Germany). The NMR spectra were obtained on Bruker AC200 or WH250 spectrometers. FAB-MS spectra were obtained on Concept 1H (Krotos, Manchester, UK) with *m*-nitrobenzylic alcohol as matrix, whereas the ES-MS spectra were obtained on a HP-59987A (Hewlett Packard) with acetonitrile as matrix.

Chemicals: The buffer solutions were prepared by titration of 0.1 M KH_2PO_4 with 0.1 M K_2HPO_4 or 0.1 M H_3PO_4 solutions and the pH was adjusted with the aid of a pH 537 pH meter with glass electrode E56 (WTW). 1,10-Phenanthroline-5,6-dione (PD) [20], trispyridylmethylamine (TPA) [21], and the complexes $[Ru(Cl)_3(DMSO)_3]$ [22], $[Co(phen)_3](BF_4)_2$ [23], $[Co(PD)_3](BF_4)_2$ [24], and $[Ru(PD)_3](ClO_4)_2$ [25] were synthesized according to described methods.

The pH-dependent studies of the redox potentials were carried out by dissolving the substrate in acidic phosphate buffer (0.1 M) and titration under pH control with 0.1 M NaOH.

PDMe(BF_4): 1,10-Phenanthroline-5,6-dione (200 mg, 0.95 mmol) was dissolved in dry dichloromethane (50 mL), and this solution was added dropwise to a suspension of $(CH_3)_3OBF_4$ (1.5 mmol, 215 mg) in dry dichloromethane (100 mL). The solution was stirred for 2 h, and the ppt was filtered off and recrystallized from acetonitrile/dichloromethane, yielding 77% (228 mg, 0.73 mmol) of the desired compound. ^1H NMR (250 MHz, CD_3CN): $\delta = 9.15$ (dd, 1H, $J = 4.3$; 2.3 Hz), 9.10 (dd, 1H, $J = 7.6$; 1.1 Hz), 9.02 (dd, 1H, $J = 6.6$; 1.1 Hz), 8.59 (dd, 1H, $J = 7.0$; 2.3 Hz), 8.18 (dd, 1H, $J = 7.6$; 6.6 Hz), 7.87 (dd, 1H, $J = 7.0$; 4.3 Hz), 4.92 (s, 3H); ^{13}C NMR (62.9 MHz, CD_3CN): $\delta = 177.2$, 176.1, 155.0, 154.4, 148.0, 145.3, 142.2, 138.2, 132.8, 131.0, 128.5, 128.2, 54.2; FAB-MS (*m*-NBA), *m/z* (%) [assignment]: 277.1 (44) $[M + 2\ddot{U} - BF_4]^+$, 243.0 (2) $[M + H_2O - BF_4]^+$, 378.1 (16) $[M + m\text{-NBA} - BF_4]^+$, 531.1 (1) $[M + 2m\text{-NBA} - BF_4]^+$. The $[M]^+$ peak was not detected; only the molecular ion in combination with the matrix could be found; IR (KBr): 1727, 1708, 1571, 1060, 726 cm^{-1}; $C_{13}H_9N_2O_2BF_4$ (312.03): calcd C 50.04, H 2.91, N 8.98; found C 49.89, H 3.16, N, 8.84.

[Co(TPA)(PD)](BF_4)$_2$: $CoCl_2 \cdot 6H_2O$ (476 mg, 2 mmol) was dissolved in deaerated water (10 mL) and TPA (580 mg, 2 mmol) was added. The blue solution was stirred for 1 h. To this solution of a paramagnetic trigonal bipyramidal complex PD (420 mg, 2 mmol) was added. The dark green solution was stirred for 1 h and the complex was precipitated by adding aqueous sodium tetrafluoroborate. The crude material was recrystallized from acetone/ether to give 89% (1.33 g, 1.78 mmol) of the desired compound. ^1H NMR: (CD_3CN, 200 MHz) for [Co(TPA)Cl]Cl: $\delta = 132.8$ (s, 3H), 108.9 (s, 6H), 57.5 (s, 3H), 47.8 (s, 3H), −2.0 (s, 3H); $C_{30}H_{24}N_6O_2CoB_2F_8 \cdot H_2O$ (751.12): calcd C 47.97, H 3.49, N 11.19, found C 47.81, H 3.31, N 10.91.

[Ru(TPA)(PD)]Cl$_2$: $[Ru(Cl)_3(DMSO)_3]$ (100 mg, 0.22 mmol) and TPA (66 mg, 0.22 mmol) were stirred for 1 h in methanol (5 mL). After the solution became reddish brown (quantitative transformation detected by ^1H and ^{13}C NMR), PD (1.5 equiv, 72 mg, 0.34 mmol) was added. The solution was refluxed for 6 h, then the solvent was removed and the residue was dissolved in water. This solution was then washed with dichloromethane to remove the uncomplexed ligand. The water was distilled off and the ppt was recrystallized twice from acetone/ether to yield the complex in 66% yield (101 mg, 0.15 mmol). The substance is very hygroscopic and has to be stored in vacuo. IR (KBr): 1698, 1605, 1560, 1425, 1293, 1015, 942, 813, 770, 722, 563 cm^{-1}; ES-MS (CH_3CN): *m/z* = 637.1 $[Ru(TPA)(PD)Cl]^+$; $C_{30}H_{24}N_6O_2RuCl_2 \cdot 10H_2O$ (852.69): calcd C 42.26, H 5.20, N, 9.86, found: C 42.58, H 4.45, N 9.91.

Acknowledgements: Financial support by the Deutsche Forschungsgemeinschaft (DFG Ste-227/18-1), the European Community through the HCMR program (CHRX-CT92-0073), NATO through a collaborative research grant (CRG910871), the Fonds der Chemischen Industrie, BASF AG, a

graduation fellowship (G. H.) from the state of Nordrhein-Westfalen, and a visiting scholarship (T. J.) from the German Academic Exchange Service (DAAD) are gratefully acknowledged.

Received: August 7, 1996 [F435]

[1] V. Alphand, A. Archelas, M. Frede, M. Hofbauer, K.-H. van Pée, T. Pohl, E. Steckhan, in *Enzyme Catalysis in Organic Synthesis—A Comprehensive Handbook, Vol. 2* (Eds.: K. Drauz, H. Waldmann), VCH, Weinheim, **1995**, ch. B.6.

[2] a) F. P. Guengerich, *Mammalian Cytochromes P-450, Vols. 1 and 2*, CRC, Boca Raton, **1987**; b) F. S. Sariaslani, *Critical Reviews in Biotechnology* **1989**, *9*, 171; reviews in *Cytochrome P-450: Advances and prospects. FASEB J.* **1992**, *6*, 667–792.

[3] a) D. T. Gibson, M. Hensley, H. Yoshioka, T. S. Mabry, *Biochemistry* **1970**, *9*, 1626; b) T. Hudlicky, H. Luna, H. F. Olivo, C. Andersen, T. Nugent, J. D. Price, *J. Chem. Soc. Perkin Trans. 1* **1991**, 2907; c) S. Ley, M. Parra, A. J. Redgrave, F. Sternfeld, *Tetrahedron* **1990**, *46*, 4995.

[4] a) W.-D. Fessner, G. Sinerius, *Angew. Chem.* **1994**, *106*, 217; *Angew. Chem. Int. Ed. Engl.* **1994**, *33*, 209; b) E. Steckhan, *Top. Curr. Chem.* **1994**, *170*, 99.

[5] J. B. Jones, E. Jakovac, *Org. Synth.* **1985**, *63*, 10.

[6] a) H. G. Davies, R. H. Green, D. R. Kelly in *Biotransformations in Preparative Organic Chemistry*, Academic Press, London, **1989**, ch. 4; b) J. B. Jones, C. J. Sih, D. Perlman, *Applications of Biochemical Systems in Organic Synthesis*, in *Techniques of Chemistry, Vol. X, Part II*, Wiley, New York, **1976**; c) K. Nakamura, M. Aizawa, O. Miyawaki, *Electroenzymology, Coenzyme Regeneration*, Springer, Berlin, **1988**.

[7] a) A. Fassoune, J. M. Laval, J. Moiroux, *Biotechnol. Bioeng.* **1990**, *35*, 935; b) J. M. Laval, C. Bourdillon, J. Moiroux, *ibid.* **1987**, *30*, 157; c) J. Bonnefoy, J. Moiroux, J. M. Laval, C. Bourdillon, *J. Chem. Soc. Faraday Trans. 1* **1988**, *84*, 941.

[8] a) J. B. Jones, K. E. Taylor, *J. Chem. Soc. Chem. Commun.* **1973**, 205; b) J. B. Jones, K. E. Taylor, *Can. J. Chem.* **1976**, *54*, 2969; *ibid.* 2974.

[9] a) S. Itoh, M. Kunigawa, N. Mita, Y. Ohshiro, *J. Chem. Soc. Chem. Commun.* **1989**, 694; b) S. Itoh, N. Mita, Y. Ohshiro, *Chem. Lett.* **1990**, 1949; c) M. Frede, Ph.D. thesis, Bonn, **1993**.

[10] a) H. Huck, H. L. Schmidt, *Angew. Chem.* **1981**, *93*, 421; *Angew. Chem. Int. Ed. Engl.* **1981**, *20*, 402; b) C. Degrand, L. L. Miller, *J. Am. Chem. Soc.* **1980**, *102*, 5728; c) N. K. Lau, L. L. Miller, *ibid.* **1983**, *105*, 5271.

[11] Preliminary results: G. Hilt, E. Steckhan, *J. Chem. Soc. Chem. Commun.* **1993**, 1706.

[12] Y. Lei, F. C. Anson, *J. Am. Chem. Soc.* **1995**, *117*, 9849.

[13] T. S. Eckert, T. C. Bruice, *J. Am. Chem. Soc.* **1983**, *105*, 4431.

[14] V. G. Levich, *Physicochemical Hydrodynamics*, Prentice-Hall, Englewood Cliffs, NJ, **1962**, pp. 345–57.

[15] W. Vielstich, D. Jahn, *Z. Elektrochem.* **1958**, *32*, 2437.

[16] Y. Lei, C. Shi, F. C. Anson, *Inorg. Chem.* **1996**, *35*, 3044.

[17] a) H. Bock, P. Hänel, *Z. Naturforsch.* **1992**, 47b, 288; b) D. M. Adams, B. Li, J. D. Simon, D. N. Hendrickson, *Angew. Chem.* **1995**, *107*, 1580; *Angew. Chem. Int. Ed. Engl.* **1995**, *34*, 1481.

[18] G. Hilt, E. Steckhan, unpublished results.

[19] a) T. P. DeAngelis, W. R. Heineman, *J. Chem. Edu.* **1976**, *9*, 594; b) W. R. Heineman, F. M. Hawkridge, H. N. Blount, in *Electroanalytical Chemistry, Vol. 7* (Ed.: A. J. Bard), Marcel Dekker, New York, **1974**, 1.

[20] M. Yamada, Y. Tanaka, Y. Yoshimoto, S. Kuroda, I. Shimao, *Bull. Chem. Soc. Jpn.* **1992**, *65*, 1006.

[21] M. M. da Mota, J. Rodgers, S. M. Nelson, *J. Chem. Soc. A* **1969**, 2036.

[22] U. C. Sarma, K. P. Sarma, R. K. Poddar, *Polyhedron* **1988**, *7*, 1727.

[23] P. Pfeiffer, B. Werdelmann, *Z. Anorg. Allg. Chem.* **1950**, *261*, 197.

[24] C. A. Goss, H. D. Abruna, *Inorg. Chem.* **1985**, *24*, 4263.

[25] This complex was synthesized in the same manner as described for $[Co(PD)_3](BF_4)_2$ except that $CoCl_2$ is replaced by $[Ru(Cl)_3](DMSO)_3]$ and precipitation is carried out with saturated $LiClO_4$ solution.

 0947-6539/97/0301-0088 $ 15.00+.25/0